

Polymerization of methyl methacrylate in ternary oil-in-water microemulsions

L. M. Gan*, C. H. Chew and K. C. Lee

Department of Chemistry, National University of Singapore, Singapore 0511, Republic of Singapore

and S. C. Ng

Department of Physics, National University of Singapore, Singapore 0511, Republic of Singapore

(Received 23 April 1992; revised 20 October 1992)

Polymerization of methyl methacrylate has been studied in ternary o/w microemulsions that were stabilized by stearyltrimethylammonium chloride. The latices produced still remain transparent and stable about one year after preparation. It is calculated that each small latex particle of hydrodynamic radius (R_h) ranging from 20 to 24 nm contained two or three polymer chains of high molecular weight of 5 to 8 million. The rate of polymerization shows only two intervals for most of the systems. This corresponds to the rates of nucleation and growth of particles. But a constant rate of polymerization is also noted for the first time for microemulsions containing a lower concentration of initiator and/or at a lower temperature ($T < 55^\circ\text{C}$). A possible mechanism related to rates of free-radical generation and polymerization is proposed to explain this constant rate of polymerization in a microemulsion.

(Keywords: polymerization; methyl methacrylate; microemulsion; kinetics)

INTRODUCTION

Work on microemulsions has been quite extensive since the first report by Hoar and Schulman¹ in 1943. Microemulsion polymerizations of methyl methacrylate (MMA) and methyl acrylate (MA) were first reported by Stoffer and Bone^{2,3} only in 1980, but the systems were unstable during polymerization, resulting in phase separation. However, Leong and Candau^{4,5} successfully polymerized acrylamide in a stable inverse water-in-oil (w/o) microemulsion. Atik and Thomas⁶ reported the success of an oil-in-water (o/w) microemulsion polymerization of styrene, producing spherical and monodisperse latex particles. Since then, several other researchers⁷⁻¹² have also studied the polymerizations of styrene and MMA in different o/w microemulsions. From the kinetic investigation of styrene polymerization in o/w microemulsions, Guo *et al.*^{13,14} showed that there are two intervals with different rates of polymerization, which relate to particle nucleation and growth. Microemulsion polymerization of styrene and/or MMA has also been studied using pulsed u.v. laser initiation¹⁵, photo-redox-induced polymerization¹⁶ and Raman spectroscopy¹⁷. Copolymerizations of MMA with acrylamide and styrene with acrylamide were also carried out in inverse microemulsions¹⁸⁻²⁰.

The above-cited polymerizations of styrene and MMA have been carried out in o/w microemulsions containing a cosurfactant. The most commonly used cosurfactant was pentanol, followed by hexanol⁶ and butyl carbitol^{10,11}. A suitable ternary system without a

cosurfactant would be more desirable for studying the kinetics of microemulsion polymerization. Pérez-Luna *et al.*²¹ reported the polymerization of styrene in three-component cationic microemulsions using dodecyltrimethylammonium bromide (DTAB). The size control of polystyrene latices via a ternary microemulsion polymerization has only been discussed very recently by Antonietti *et al.*²². They also used cationic surfactants DTAB and cetyltrimethylammonium chloride (CTAC) to stabilize the microemulsions.

This paper discusses the kinetics of MMA polymerization in ternary microemulsions. A long alkyl-chain cationic surfactant, stearyltrimethylammonium chloride, was used to stabilize the system.

EXPERIMENTAL

Materials

Stearyltrimethylammonium chloride (STAC) and 2,2'-azobisisobutyronitrile (AIBN) were from Tokyo Chemical Industry. Methyl methacrylate (Fluka) was vacuum distilled at 2.5 Torr and 21°C. STAC was recrystallized from an ethanol-acetone mixture (1:3 by volume). Potassium persulfate (KPS) and AIBN were recrystallized from doubly distilled water and methanol respectively. Standard polystyrenes of known molecular weights and polystyrene latices of known particle sizes were obtained from Polyscience Inc.

Phase diagram of microemulsion

The clear o/w microemulsion regions were determined visually at room temperature by titration of water into

* To whom correspondence should be addressed

culture tubes (with caps) containing different amounts of surfactant and MMA mixtures. The stable microemulsion regions after polymerization were established by polymerizing MMA with 0.6 mM KPS or 0.6 mM AIBN in a series of sealed ampoules at 60°C.

Polymerization

The dilatometric method was used to study the kinetics of microemulsion polymerization. The dilatometer consisted of a 10 ml Erlenmeyer flask with an attached 40 cm long capillary 2 mm in diameter. The microemulsion in a ground-glass tube was first frozen by liquid nitrogen and degassed at about 10 Torr for one freeze-thaw cycle. It was then introduced directly into the dilatometer through a special joint attachment and placed in a thermostated bath. The change of liquid level in the capillary of the dilatometer was monitored by a cathetometer as a function of time. The polymer conversion was calculated from the volume change of liquid in the capillary.

Particle size determination

Particle sizes of microemulsion latices were determined using a Malvern 4700 light scattering spectrophotometer. Prior to measurements, the microemulsion latices were diluted with a critical micelle concentration (c.m.c.) solution of the surfactant until the volume fractions of particles were in the range of 0.01 to 0.1. Polystyrene latex of known size was used as a standard.

Molecular-weight determination

The polymerized microemulsion latices were precipitated in a large quantity of methanol. The polymer was washed until free of the surfactant. The molecular weights of polymers were characterized by a Varian Vista 5500 liquid chromatography system with an RI-3 detector. The columns used were Varian Micropak TSK 7000H and GMH6 in series and the eluant was tetrahydrofuran (THF). Polystyrene standards in 0.2 mg ml⁻¹ THF were used for calibration. The flow rate was maintained at 0.8 ml min⁻¹.

RESULTS AND DISCUSSION

Figure 1 shows the ternary o/w microemulsion region composed of STAC, MMA and water. The microemulsions prepared within this bounded region were fluid. Most of the polymerized microemulsions appear reddish and were still stable. Those with higher concentrations of MMA and STAC, as shown by the shaded region in Figure 1, were not stable after polymerization. The stable region for polymerized microemulsions using KPS was larger than that for AIBN as indicated by the clear region extending to the boundary ab for the former and cd for the latter.

The compositions of o/w microemulsions listed in Table 1 were used for the kinetic study of polymerizations. From systems M1 to M4, the concentration of MMA was varied from 3 to 9 wt% by keeping a constant weight ratio of water to STAC at 8.1. The effects of concentrations of monomer and initiator as well as temperature on the polymerization are discussed in the following sections.

Effect of MMA concentration

The rate of polymerization was 0.92 order (first order) with respect to MMA concentration. Figure 2 shows that

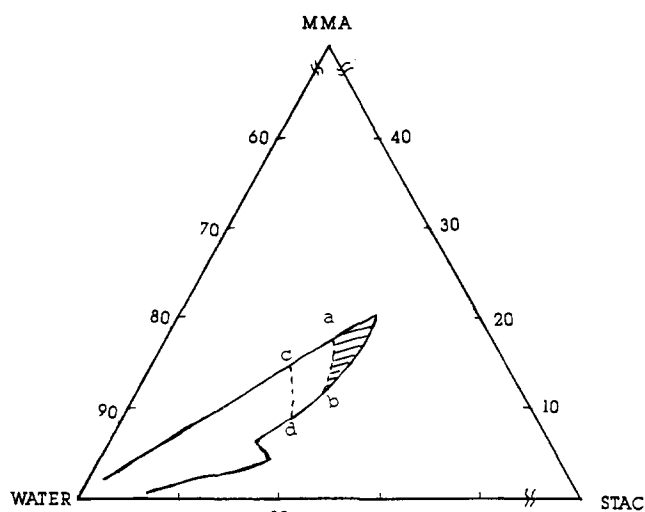


Figure 1 The phase diagram of the o/w microemulsion system at 30°C before polymerization (the whole enclosed region). The stable regions after polymerization at 60°C with 0.6 mM KPS and 1.39 mM AIBN are represented by the boundaries ab and cd respectively

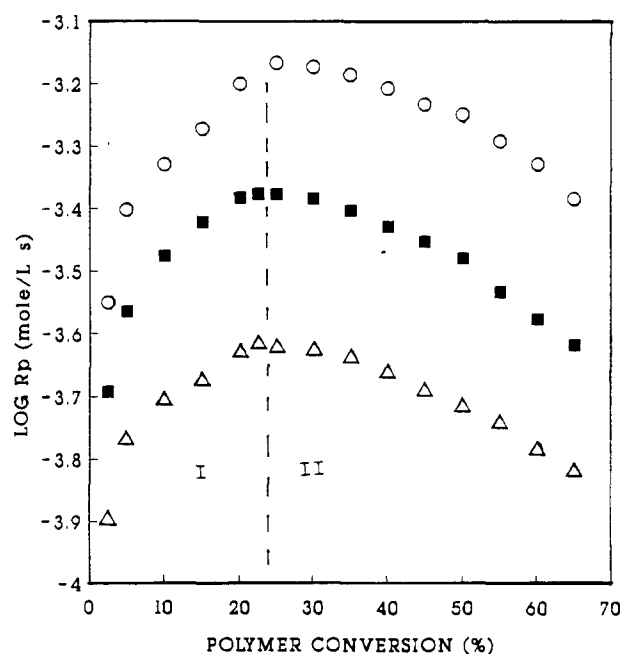


Figure 2 Effect of MMA concentration on polymerization using 0.15 mM KPS at 60°C: (Δ) 3%, (■) 5% and (○) 7% MMA

Table 1 Compositions for microemulsion polymerization of MMA

Composition (wt%)	M1	M2	M3	M4
MMA	3.0	5.0	7.0	9.0
H ₂ O	86.3	84.6	82.8	81.0
STAC	10.7	10.4	10.2	10.0
H ₂ O/STAC	8.1	8.1	8.1	8.1

[KPS] = 0.15, 0.30, 0.45 and 0.60 mM based on water
[AIBN] = 0.52, 0.87 and 1.39 mM based on water
Temp. = 55.0, 57.5, 60.0, 62.5 and 65.0°C

the overall polymerization rates increased with increasing monomer concentration. Only two polymerization rate intervals were observed, i.e. the rate increased with polymer conversion up to 20–25% in interval I and then decreased in interval II. There was no apparent constant

Table 2 Particle sizes and virial coefficients (α) of PMMA latices prepared at 60°C

System	MMA (%)	R_g (nm)	R_h (nm)	R_h/R_g	α	\bar{M}_w (10^6)	\bar{M}_w/\bar{M}_n
M1	3	8.6	19.9	2.31	-5.18	7.2	2.3
M2	5	10.4	20.9	2.00	-4.85	6.7	2.4
M3	7	11.9	22.9	1.92	-4.68	7.6	2.6
M4	9	13.7	24.2	1.77	-4.10	8.2	2.6

rate region as would be expected for a conventional emulsion polymerization due to the presence of monomer droplets.

In the interval I, the increasing rate of polymerization was a consequence of increasing number of polymerization loci, which were continuously nucleated by the free-radical flux. The interval I (nucleation period) ended after it reached the maximum polymerization rate, which began to decrease in the interval II (particle growth). This is because the monomer concentration in growing particles was diminishing.

The hydrodynamic radii of the latices ($R_h = 20\text{--}24$ nm) increased with increasing concentration of monomer as shown in Table 2. A similar trend was also observed by Pérez-Luna *et al.*²¹ for ternary styrene microemulsions. The sizes of their latices were only slightly larger than those of the unpolymerized microemulsion droplets, both of which were dependent on monomer concentration. However, the hydrodynamic radii (R_h) and the geometric radii (R_g) of our latices were very much different. The large disparity between R_h and R_g could be due to the thicker hydrophobic region created by the long STAC chain in the membrane phase (interface) of a latex particle.

The virial coefficient (α) was obtained from the diffusion coefficient (D) of latex particles at different volume fractions (Φ) by light scattering measurements, i.e. $D = D_0(1 + \alpha\Phi)$. The relative value of α is an indication of interaction between latex particles. A more negative value of α implies a smaller repulsive interaction between the particles. This means that the particles may approach closer to each other or even penetrate into the stabilized spheres of the particles. The stabilized sphere encompasses electric double layers and the surfactant membrane at the interface. Unpolymerized MMA molecules are deemed to be present also in the interfacial region because MMA is rather polar and its solubility in the aqueous phase is as high as 1.56 wt%²³. Even the polymerized microemulsions always contained some unpolymerized MMA as the maximum polymer conversions were always around 96–97%. System M1 containing the least amount of MMA (3%) showed the largest negative value of α (-5.18), while system M4 containing the largest amount of MMA (9%) exhibited the smallest negative value of α (-4.10). The geometric radius (R_g) is related to the size of the polymer, which was mainly present in the core and only a small fraction of it in the membrane phase of a latex particle. The ratio R_h/R_g decreased from 2.31 to 1.77 with increase of the MMA content from 3 to 9%. As indicated by the less negative value of α , latex particles progressively became less penetrable into their stabilized spheres owing to the formation of more polymer in the membrane phase at higher MMA concentrations. This is because the monomer concentration in the membrane phase would increase with increase of total monomer

concentration in the system, as was found in the styrene microemulsion²⁴.

All molecular weights of PMMA were found to be in the range of 7.2×10^6 to 8.2×10^6 with a slight dependence on monomer concentration. The polydispersity indices (PDI) also increased marginally from 2.3 to 2.6 as the MMA content was increased from 3 to 9%.

Effect of KPS concentration

The effect of KPS concentration on the initial rate of polymerization of 9% MMA at 60°C (R_p at 2.5% conversion) is shown in Figure 3. The maximum rates of polymerizations appeared around 20–25% polymer conversion. As would be expected, the rate of polymerization increased with increasing KPS concentration because of the increasing number of initiated microemulsion droplets due to a larger free-radical flux. The dependence of R_p on KPS concentration was found to be 0.48 power, which was also observed in styrene microemulsion polymerization¹⁰.

With 1.56 wt% MMA (1.56×10^{-4} mol l⁻¹) dissolved in the aqueous phase of a microemulsion, it is highly probable that a fraction of the dissolved MMA would be initiated by KPS free radicals to form anion-oligomer radicals of higher hydrophobicities. A minimum addition of two or three monomer units would be necessary to impart reasonable surface activity²⁵ of an oligomer

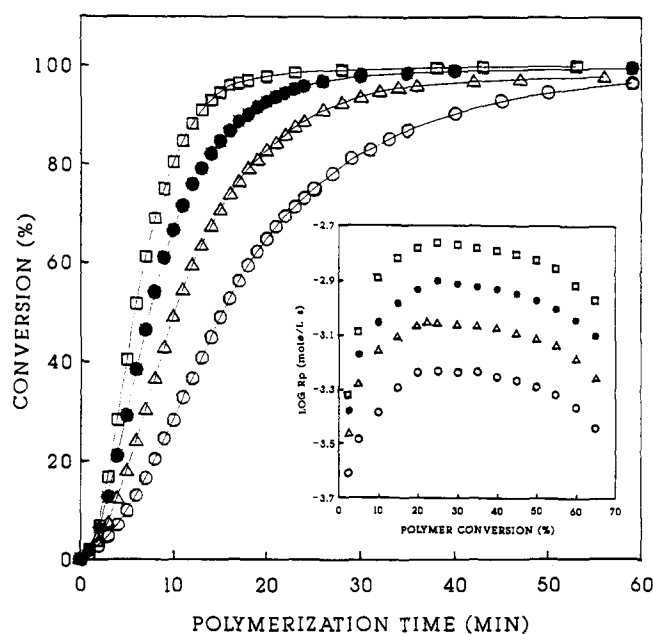

Figure 3 Effect of KPS concentration on microemulsion polymerization of 9 wt% MMA at 60°C: (○) 0.15 mM, (△) 0.30 mM, (●) 0.45 mM and (□) 0.60 mM KPS

Table 3 Effect of KPS concentration on particle size of latices and molecular weights of PMMA prepared with 9 wt% MMA at 60°C

[KPS] (mM)	R_g (nm)	R_h (nm)	N_d (10^{18} l^{-1})	\bar{M}_w (10^6)	\bar{M}_w/\bar{M}_n	N_p
0.15	13.7	24.6	2.88	8.21	2.59	2.3
0.30	13.5	23.4	3.37	7.09	2.06	2.3
0.45	13.3	23.2	3.43	—	—	—
0.60	12.5	22.2	3.94	5.97	2.75	2.3

radical. These radicals might then diffuse into microemulsion droplets to continue the polymerization. The direct entry of KPS free radicals into microemulsion droplets is also possible. But the rate of radical entry may be retarded by the condensed interfacial layer or the possibly high surface zeta-potentials in the o/w microemulsion systems²⁶.

Table 3 shows that R_h decreased, while number of latex particles per litre (N_d) increased, with increasing KPS initiator concentration, as would be expected. N_d was calculated to be in the order of 10^{15} based on the volume fraction of particles (Φ) and R_h , i.e. $\Phi = \frac{4}{3}\pi R_h^3 N_d$. The dependence of N_d on KPS concentration was only 0.23 power as compared to 0.40 for the microemulsion polymerization of styrene¹³. High molecular weights ($(6-8) \times 10^6$) coupled with low KPS concentration dependence might be due to low rates of free-radical adsorption and desorption. This led to a relatively narrow distribution of molecular weights (\bar{M}_w/\bar{M}_n), which varied from 2.1 to 2.8. Knowing N_d and \bar{M}_w , the number of polymer chains in each small latex particle (N_p) can be calculated from the weight of polymer in each millilitre of microemulsion. It is estimated that

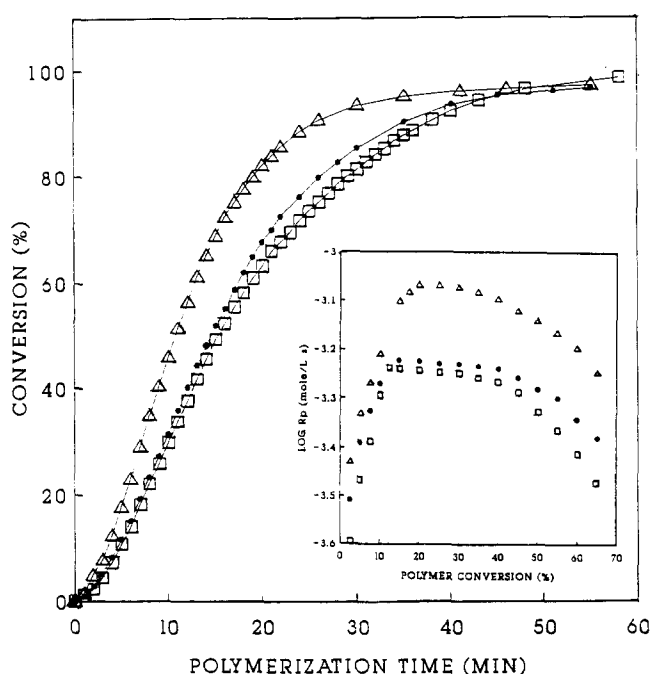


Figure 4 Effect of AIBN concentration on polymerization of 9 wt% MMA at 60°C: (□) 0.52 mM, (●) 0.87 mM and (△) 1.39 mM AIBN

each microparticle of latex contained two or three PMMA chains. A similar number of N_p was also obtained for microemulsion polymerization of styrene^{13,14}. But in the inverse microemulsion polymerization of acrylamide, each latex particle consisted of only a single polymer chain as reported by Candau *et al.*^{4,5}.

Effect of AIBN concentration

The maximum polymerization rate initiated by AIBN (Figure 4) occurred around 12–20% conversion, which was slightly dependent on the concentration of AIBN. It also exhibited a rather constant rate of polymerization in the region between 20 and 40% conversion for systems with less than 1 mM AIBN. The observation of this constant rate period in microemulsion polymerization is believed to be reported for the first time.

Table 4 summarizes the information for systems initiated by KPS and AIBN. The rates of polymerization were much higher for the KPS-initiated systems than those of AIBN at equal concentrations of initiators. Based on the decomposition rate constants²⁷ (k_d) of $3.16 \times 10^{-6} \text{ s}^{-1}$ for KPS in 0.1 M NaOH solution and $9.80 \times 10^{-6} \text{ s}^{-1}$ for AIBN in toluene, both at 60°C, it was calculated that rates of radicals generated by 0.3, 0.45 and 0.6 mM KPS were 1.90×10^{-9} , 2.84×10^{-9} and $3.79 \times 10^{-9} \text{ mol l}^{-1} \text{ s}^{-1}$ respectively compared to 1.02×10^{-8} , 1.71×10^{-8} and $2.72 \times 10^{-8} \text{ mol l}^{-1} \text{ s}^{-1}$ generated by 0.52, 0.87 and 1.39 mM AIBN respectively. These calculations may serve as a comparison for indicating that much higher radical concentrations would be generated from AIBN systems than from KPS systems according to the compositions used as listed in Table 1. But the maximum rates of polymerization (R_p) for AIBN systems were found to be much lower than those for KPS systems (Table 4). The discrepancy is attributed to the high rate of recombination of AIBN radicals within small microemulsion droplets containing MMA. Only a very small fraction of the free radicals would successfully initiate the polymerization. On the other hand, the main source of initiation might come from AIBN radicals generated in the aqueous phase. This is because the solubility of AIBN in the continuous phase of the o/w microemulsion was $3.3 \times 10^{-2} \text{ mM}$, which could generate $6.51 \times 10^{-10} \text{ mol l}^{-1} \text{ s}^{-1}$ free radicals. These AIBN radicals would initiate polymerization just like KPS radicals. This concentration of AIBN radicals generated in the aqueous phase was one order of magnitude smaller than that of KPS used. This could be the main reason for explaining the much lower R_p for the AIBN system than that of KPS.

Table 4 Comparison between systems initiated by KPS and AIBN for 9% MMA at 60°C

I	[I] (mM)	Max. R_p ($10^{-4} \text{ mol l}^{-1} \text{ s}^{-1}$)	Max. nucleation			N_d (10^{18} l^{-1})	N_p	\bar{M}_w (10^6)
			Conv. (%)	t (min)	R_h (nm)			
KPS	0.15	6.0	17.5	6.5	24.6	2.88	2.3	8.2
	0.30	8.9	22.5	5.7	23.4	3.07	2.3	7.1
	0.45	12.6	25.0	4.5	23.2	3.43	2.9	5.5
	0.60	17.4	25.0	3.7	22.2	3.94	2.3	6.0
AIBN	0.52	5.8	12.5	6.3	25.4	2.63	3.0	6.9
	0.87	6.0	15.0	5.9	24.5	2.91	2.2	8.6
	1.39	8.5	20.0	5.5	23.7	3.22	2.3	7.5

Two sets of similar R_p from both systems (Table 4) are used for the following discussion. One of them ($6 \times 10^{-4} \text{ mol l}^{-1} \text{ s}^{-1}$) was obtained from either 0.15 mM KPS or 0.87 mM AIBN system. The other set of R_p of $8.9 \times 10^{-4} \text{ mol l}^{-1} \text{ s}^{-1}$ from 0.30 mM KPS system and $8.5 \times 10^{-4} \text{ mol l}^{-1} \text{ s}^{-1}$ from 1.39 mM AIBN system are considered to be similar. This indicates that 0.15 mM KPS and 0.87 mM AIBN or 0.30 mM KPS and 1.39 mM AIBN would produce similar effective radical concentrations during polymerizations. Consequently, their respective values of R_p , R_h , N_d , N_p and \bar{M}_w , maximum nucleation time and percentage conversion were all similar. It is thus surmised that the apparent

different characteristics of MMA polymerization initiated by KPS and AIBN are mainly due to the different efficiency in producing an effective free-radical concentration. AIBN is less efficient than KPS in producing an effective free-radical concentration for polymerization because of the high rate of mutual termination of primary radicals generated in the small volume of a microemulsion droplet. Hence R_p and N_d are less dependent on the total concentration of AIBN used. The lower dependence of R_p and N_d on AIBN concentration is found (Figure 5) to be 0.39 and 0.17 respectively compared to 0.47 and 0.23 for the KPS-initiated system.

Effect of temperature

The effect of temperature on the rate of polymerization of 9% MMA was studied using 0.15 mM KPS and 0.87 mM AIBN. The activation energies of polymerization obtained from the Arrhenius plots are 106 and 118 kJ mol^{-1} for systems initiated by KPS and AIBN respectively. Figure 6 shows the effect of temperature on the rate of polymerization of 9 wt% MMA using 0.15 mM KPS. The plots also show a rather constant rate region between 20 and 40% polymer conversion for polymerizations carried out at 55°C. However, the plateau region almost disappeared at a higher temperature of polymerization (65°C). The constant R_p region is due to a constant supply of monomer from the uninitiated microemulsion droplets to the nucleated droplets. This situation may occur only when the rate of radical generation is much slower than the rates of nucleation and growth of particles. In these circumstances, the polymerization loci continue to recruit monomer from the uninitiated microemulsion droplets, which may serve as monomer reservoirs, just like monomer droplets in emulsion polymerization. Once the rate of radical generation is increased by either increasing the concentration of the initiator or raising the temperature, a much larger fraction of microemulsion droplets would be initiated, leaving a smaller fraction of uninitiated droplets for monomer recruiting. Hence the plateau region gradually disappears.

ACKNOWLEDGEMENT

The authors are grateful to the National University of Singapore for financial support under grants RP 840038 and RP 890638.

REFERENCES

- 1 Hoar, T. P. and Schulman, J. H. *Nature* 1943, **152**, 102
- 2 Stoffer, J. O. and Bone, T. *J. Polym. Sci., Polym. Chem. Edn.* 1980, **18**, 2641
- 3 Stoffer, J. O. and Bone, T. *J. Dispersion Sci. Technol.* 1980, **1**, 37
- 4 Leong, Y. S. and Candau, F. *J. Phys. Chem.* 1982, **86**, 2269
- 5 Candau, F., Leong, Y. S. and Fitch, R. M. *J. Polym. Sci., Polym. Chem. Edn.* 1985, **23**, 193
- 6 Atik, S. S. and Thomas, J. K. *J. Am. Chem. Soc.* 1981, **103**, 4279
- 7 Tang, H. I., Johnson, P. L. and Gulari, E. *Polymer* 1984, **25**, 1357
- 8 Johnson, P. L. and Gulari, E. *J. Polym. Sci., Polym. Chem. Edn.* 1984, **22**, 3967
- 9 Jayakrishnan, A. and Shah, D. O. *J. Polym. Sci., Polym. Lett. Edn.* 1984, **22**, 31
- 10 Gan, L. M., Chew, C. H. and Lye, I. *Makromol. Chem.* 1992, **193**, 1249
- 11 Lye, I., Chew, C. H. and Gan, L. M. Preprints of papers presented at the IUPAC International Symposium, Speciality Polymers, Singapore, 1990, p. 210

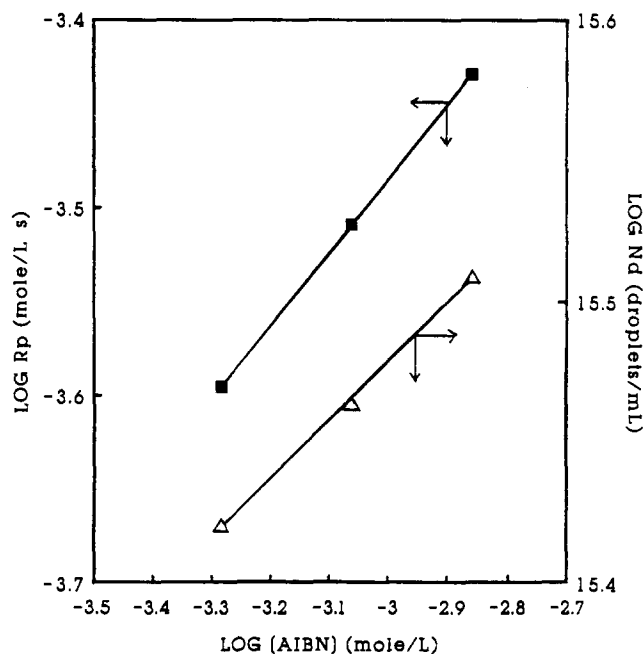


Figure 5 Effect of AIBN concentration on the rate of polymerization of 9 wt% MMA (R_p) at 60°C and the number of latex particles per millilitre (N_d)

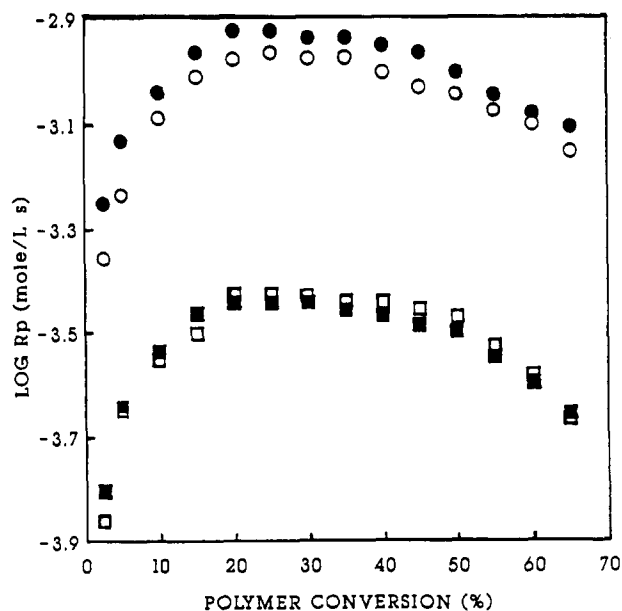


Figure 6 Effect of temperature on the rate of polymerization of 9 wt% MMA using 0.15 mM KPS and 0.87 mM AIBN: (□) 55°C (KPS), (○) 65°C (KPS), (■) 55°C (AIBN) and (●) 65°C (AIBN)

- 12 Kuo, P. L., Turro, N. J., Tseng, C. M., El-Aasser, M. S. and Vanderhoff, J. W. *Macromolecules* 1987, **20**, 1216
- 13 Guo, J. S., El-Aasser, M. S. and Vanderhoff, J. W. *J. Polym. Sci. (A) Polym. Chem.* 1989, **27**, 691
- 14 Guo, J. S., El-Aasser, M. S. and Vanderhoff, J. W. in 'Polymer Association Structures' (Ed. M. A. El-Nokaly), American Chemical Society, Washington, DC, 1989
- 15 Holdcroft, S. and Guillet, J. E. *J. Polym. Sci. (A) Polym. Chem.* 1990, **28**, 1823
- 16 Grätzel, C. K., Jirousek, M. and Grätzel, M. *Langmuir* 1986, **2**, 292
- 17 Feng, L. and Ng, K. Y. S. *Macromolecules* 1990, **23**, 1048
- 18 Vaskova, V., Juranicova, V. and Barton, J. *Makromol. Chem.* 1990, **191**, 717
- 19 Vaskova, V., Juranicova, V. and Barton, J. *Makromol. Chem.* 1991, **192**, 989
- 20 Vaskova, V., Juranicova, V. and Barton, J. *Makromol. Chem.* 1991, **192**, 1339
- 21 Pérez-Luna, V. H., Puig, J. E., Castano, V. M., Rodriguez, B. E., Murthy, A. K. and Kaler, E. W. *Langmuir* 1990, **6**, 1040
- 22 Antonietti, M., Bremser, W., Muschenborn, D., Rosenauer, C., Schupp, B. and Schmidt, M. *Macromolecules* 1991, **24**, 6636
- 23 Riddick, A. J., Bunger, W. B. and Sakano, J. K. (Eds.) 'Organic Solvents', 4th Edn., Wiley-Interscience, New York, 1986, Vol. II, p. 423
- 24 Guo, J. S., El-Aasser, M. S., Sudol, D. E., Yue, H. J. and Vanderhoff, J. W. *J. Colloid Interface Sci.* 1990, **140**, 175
- 25 Napper, D. H., Gilbert, R. G., Maxwell, L. A. and Morrison, B. R. Preprints of International Symposium on Polymeric Microspheres, Fukui, Japan, 1991
- 26 Guo, J. S., Sudol, D. E., Vanderhoff, J. W. and El-Aasser, M. S. *J. Polym. Sci. (A) Polym. Chem.* 1992, **30**, 703
- 27 Brandrup, J. and Immergut, E. H. (Eds.) 'Polymer Handbook', 3rd Edn., Wiley, New York, 1989, p. II-57